# Supporting information

## Atomic layered metal-organic framework on NiFe LDH for enhanced electrocatalytic oxygen evolution reaction

Dan Xu,‡[a] Yingying Gao,‡[a] Sheng Qian,[a] Yu Fan,[a] Jingqi Tian*[a]

[a] *School of Chemistry and Chemical Engineering, and Institute for Innovative Materials and Energy, Yangzhou University, 180 Si-Wang-Ting Road, Yangzhou 225002, P. R. China*

*Corresponding author.

*E-mail address:* tianjq@yzu.edu.cn (J. Tian)

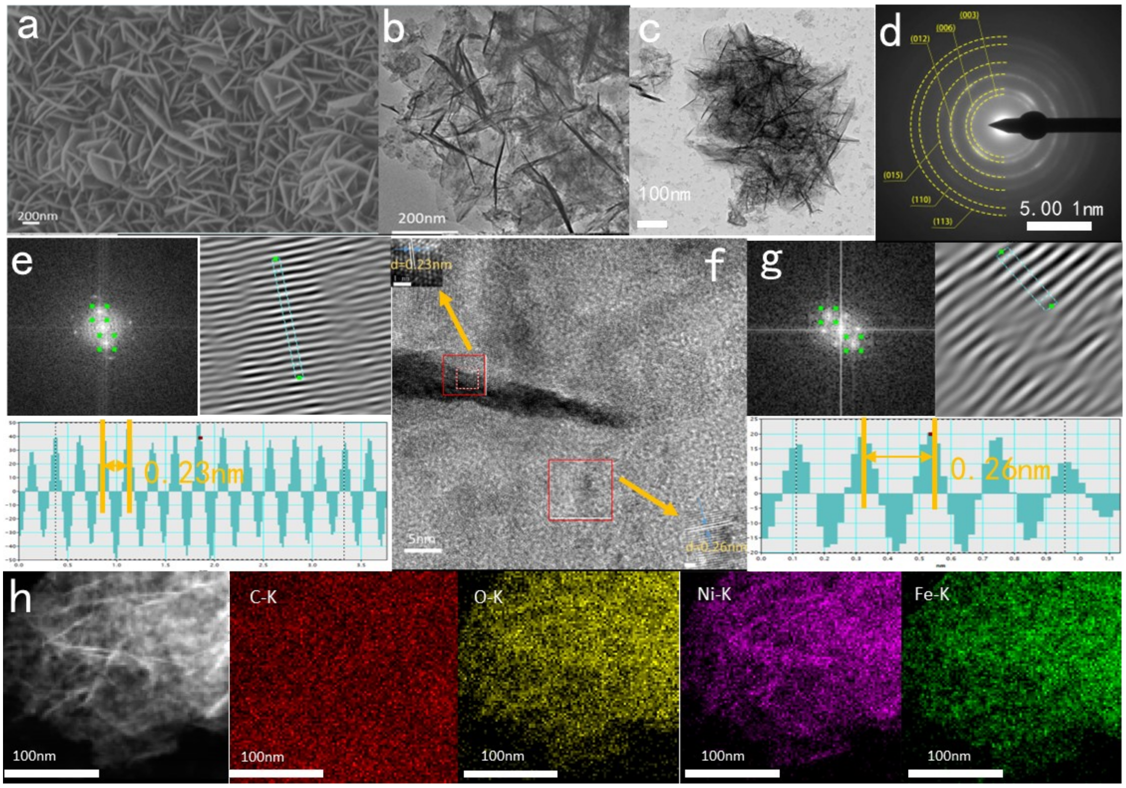


**Fig. S1.** (a) SEM image, (b, c) TEM image, (d) SAED image, (e-g) HRTEM images, (h) STEM image and elemental mappings of NiFe LDH nanosheets.

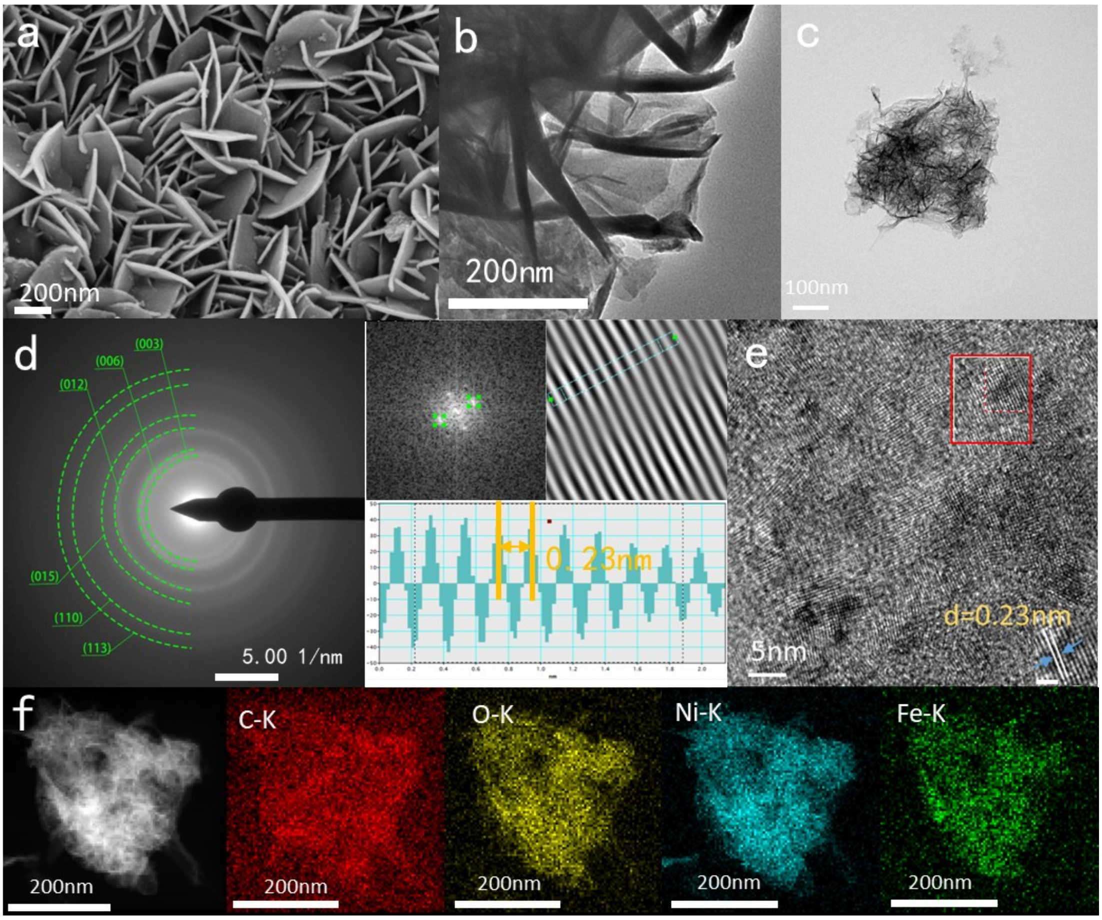


**Fig. S2.** (a) SEM image, (b, c) TEM image, (d) SAED image, (e-g) HRTEM images, (h) STEM image and elemental mappings of NiFe LDH@MOF-1.

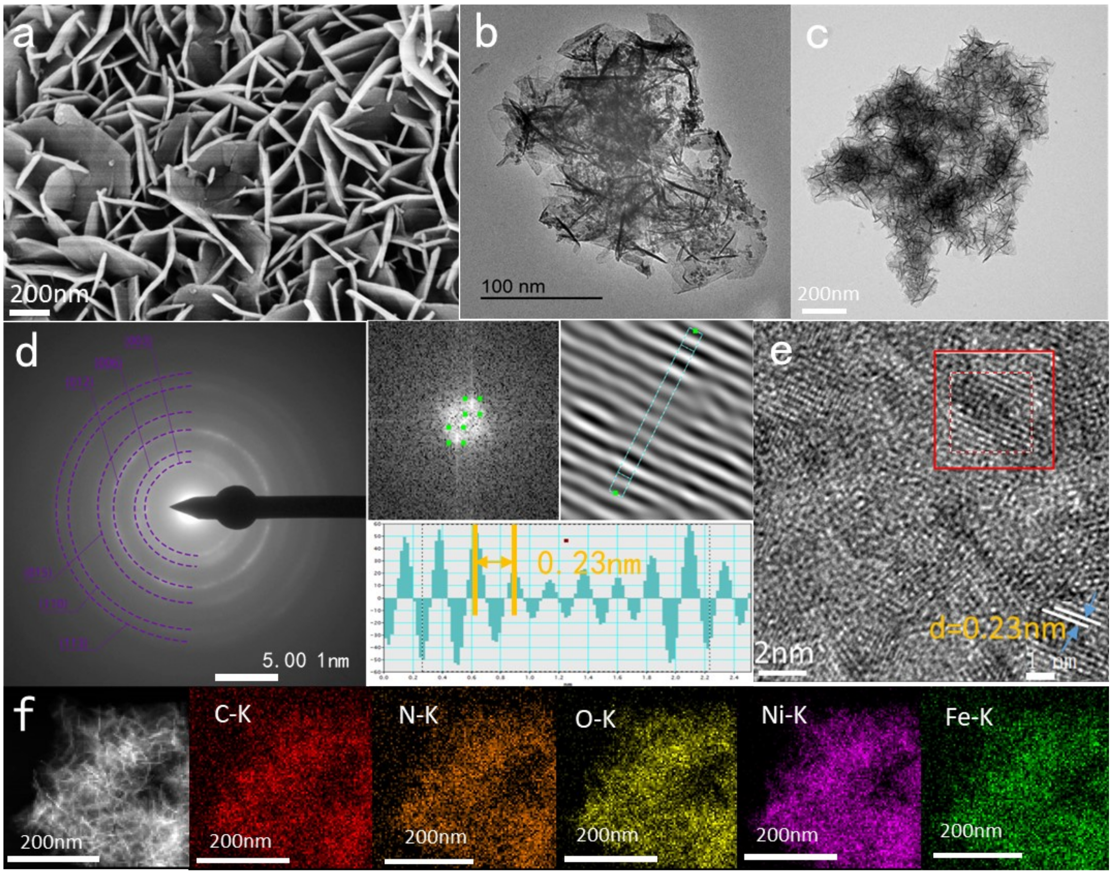


**Fig. S3.** (a) SEM image, (b, c) TEM image, (d) SAED image, (e-g) HRTEM images, (h) STEM image and elemental mappings of NiFe LDH@MOF-2.

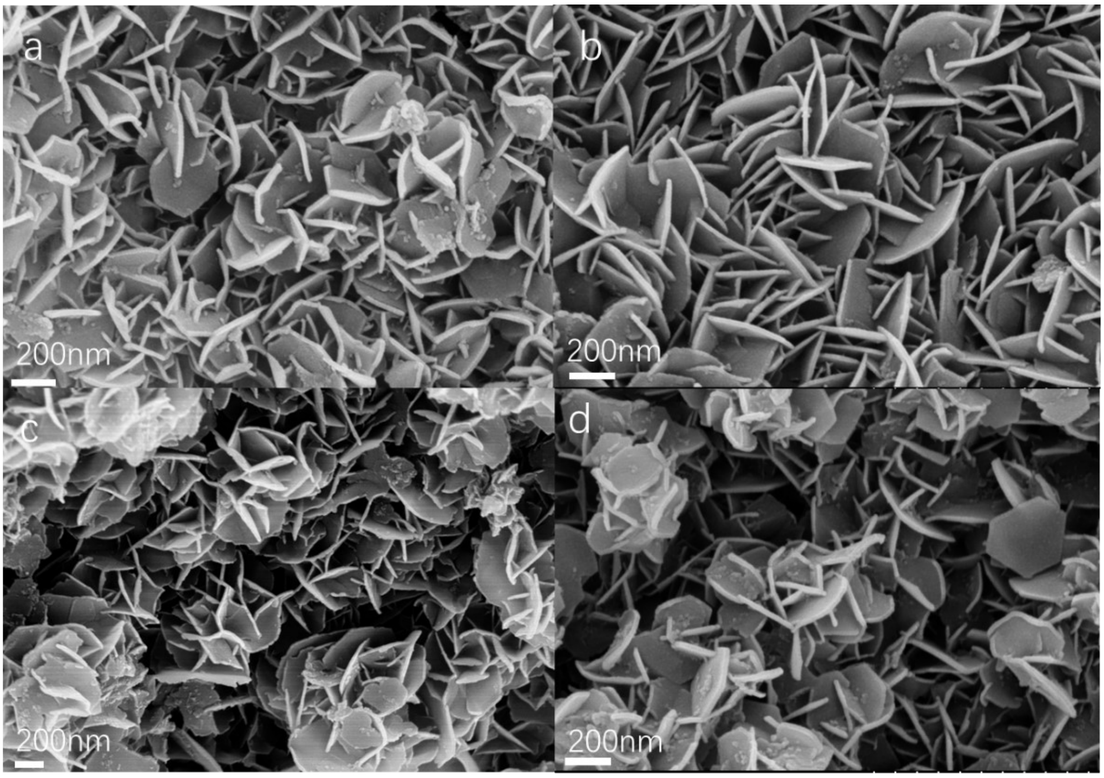

**Fig. S4.** SEM image of NiFe LDH@MOF-1 obtained at different coordination reaction period. (a) 6 h, (b) 8 h, (c) 10 h, and (d) 12 h.

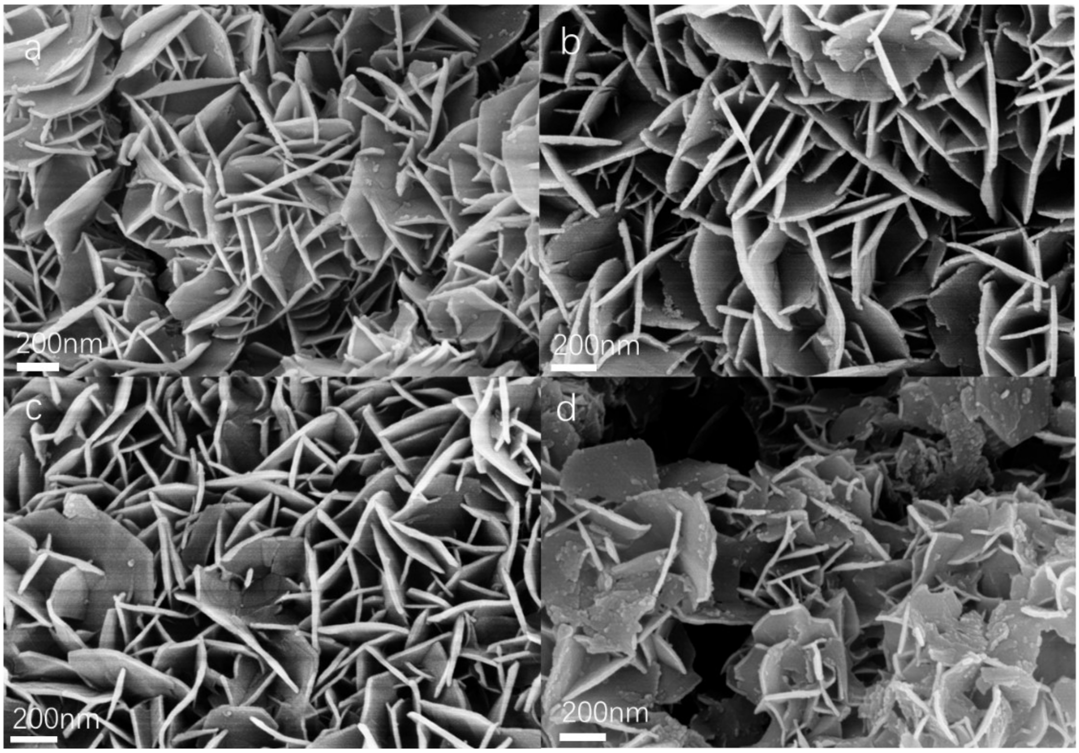

**Fig. S5.** SEM image of NiFe LDH@MOF-2 obtained at different coordination reaction period. (a) 6 h, (b) 8 h, (c) 10 h, and (d) 12 h.

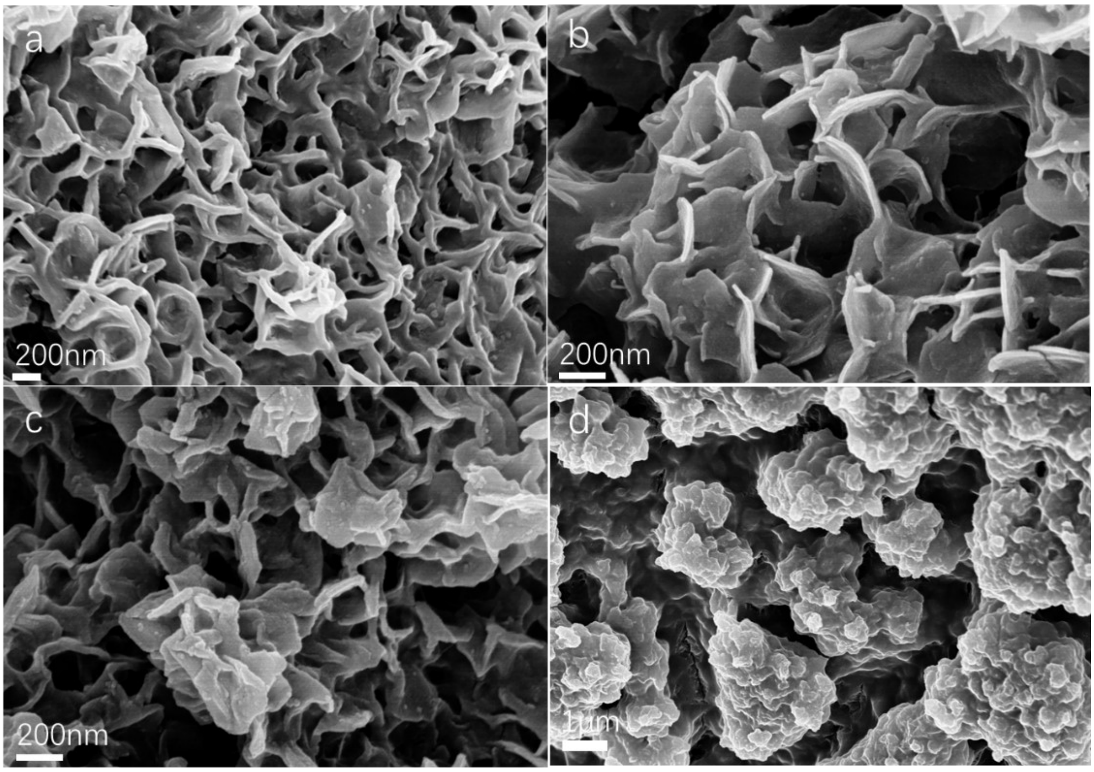


**Fig. S6.** SEM image of NiFe LDH@MOF-3 obtained at different coordination reaction period. (a) 6 h, (b) 8 h, (c) 10 h, and (d) 12 h.

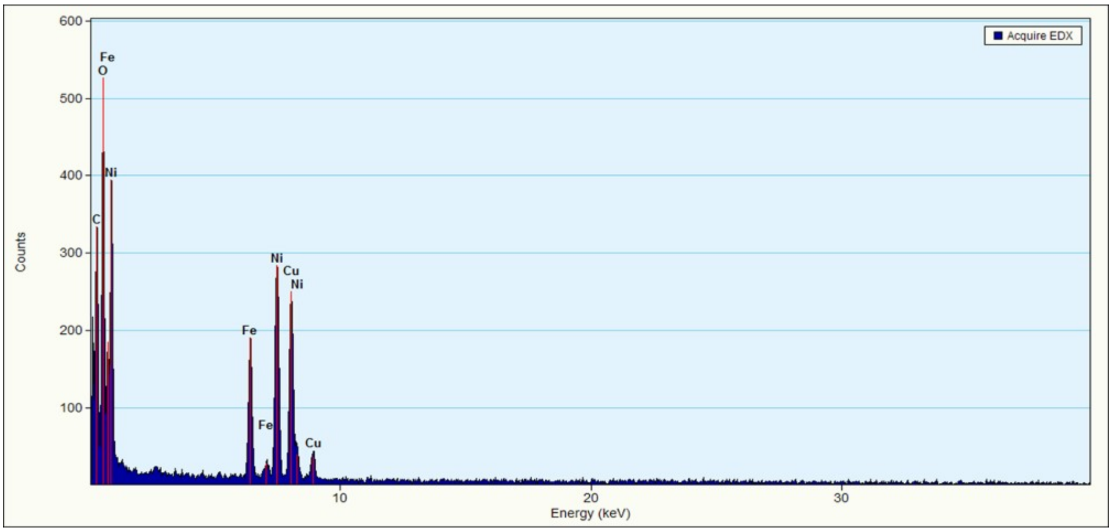

**Fig. S7.** EDX spectrum of NiFe LDH.

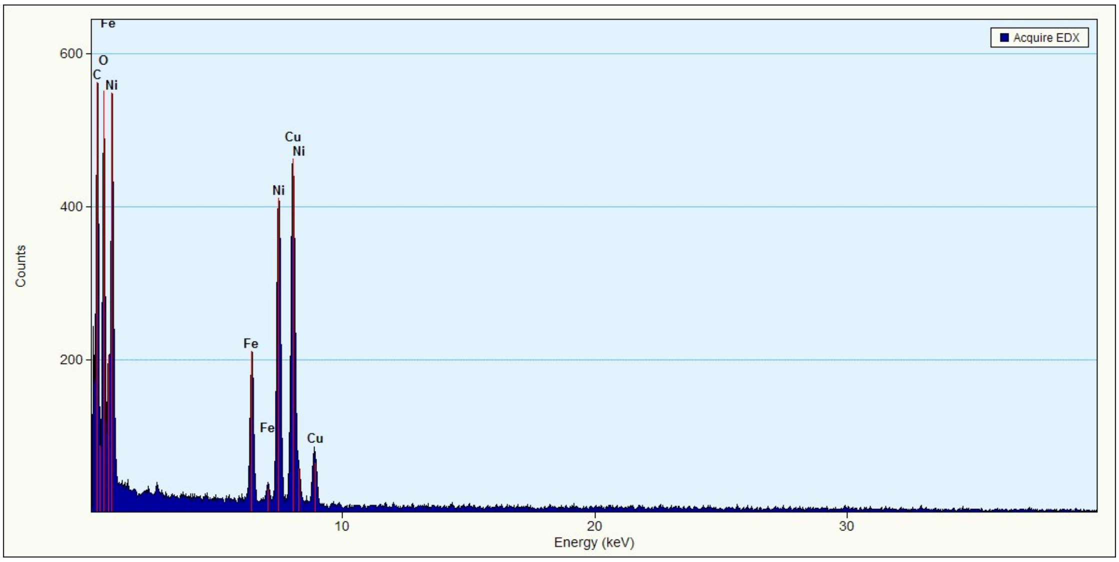


**Fig. S8.** EDX spectrum of NiFe LDH@MOF-1.

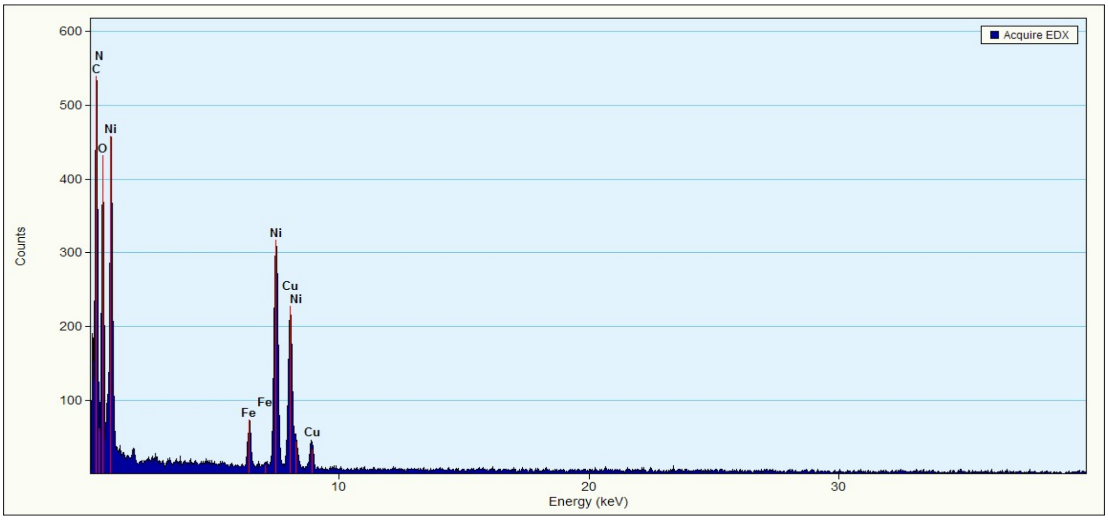

**Fig. S9.** EDX spectrum of NiFe LDH@MOF-2.

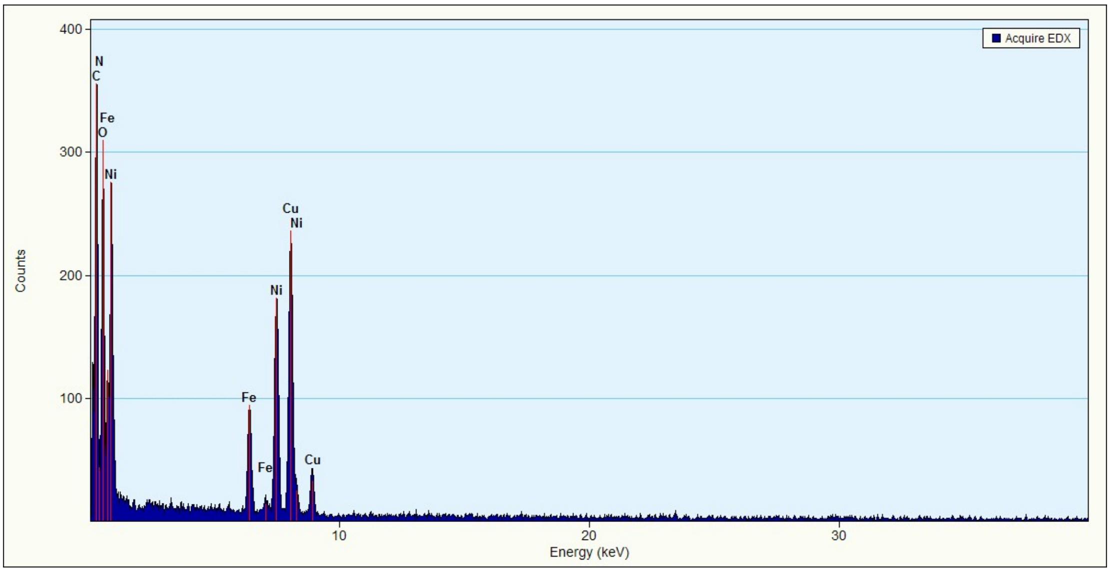

**Fig. S10.** EDX spectrum of NiFe LDH@MOF-3.

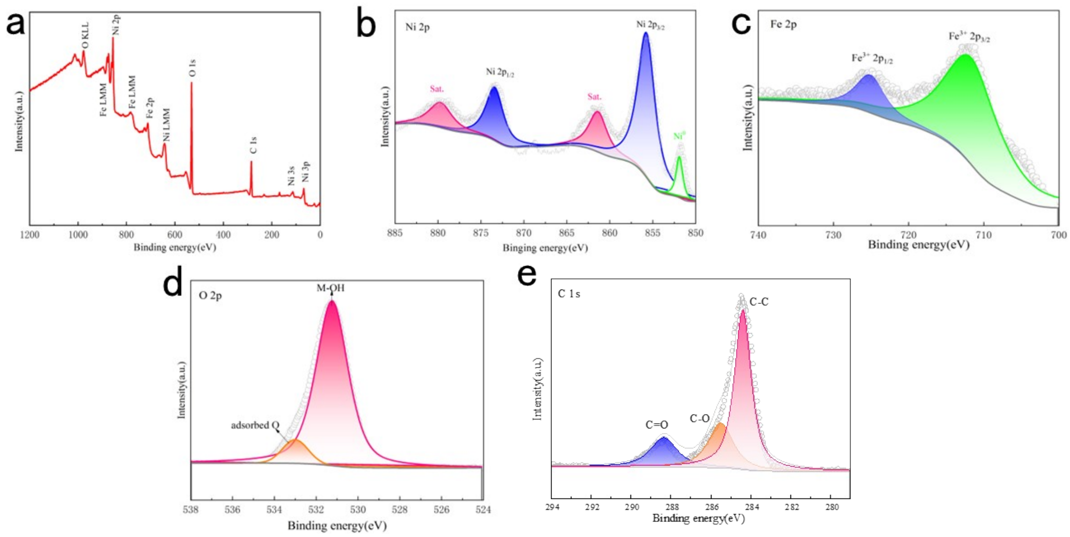


**Fig. S11.** High-resolution XPS spectra of the NiFe LDH (a) Survey spectrum, (b) Ni 2p, (c) Fe 2p, (d) O 1s, (e) C 1s.

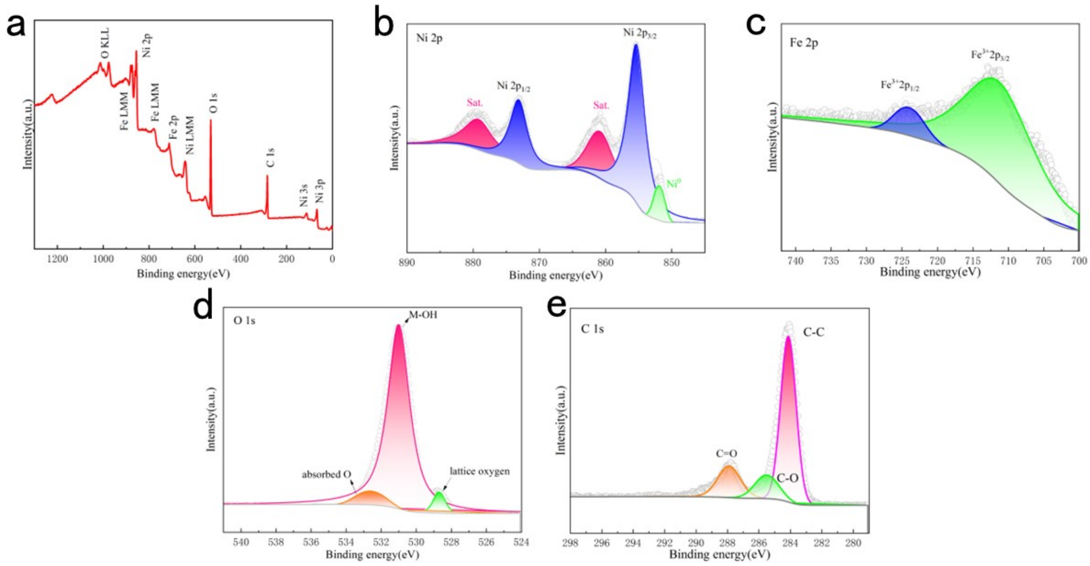


**Fig. S12.** High-resolution XPS spectra of the NiFe LDH@MOF-1 (a) Survey spectrum, (b) Ni 2p, (c) Fe 2p, (d) O 1s, (e) C 1s.

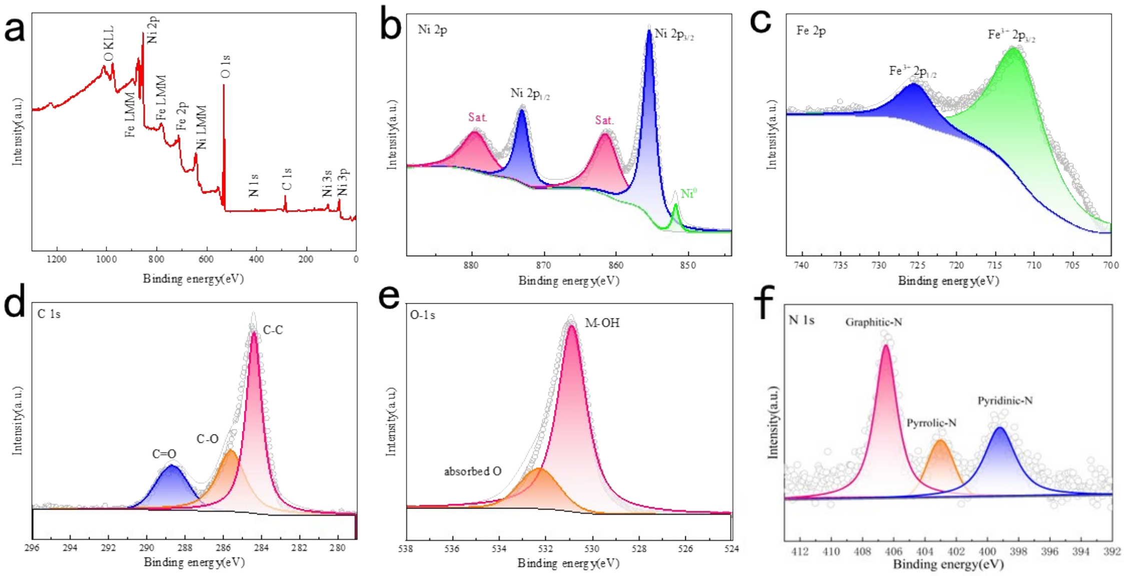


**Fig. S13**. High-resolution XPS spectra of the NiFe LDH@MOF-2 (a) Survey spectrum, (b) Ni 2p, (c) Fe 2p, (d) C 1s, (e) O 1s, (f) N 1s.

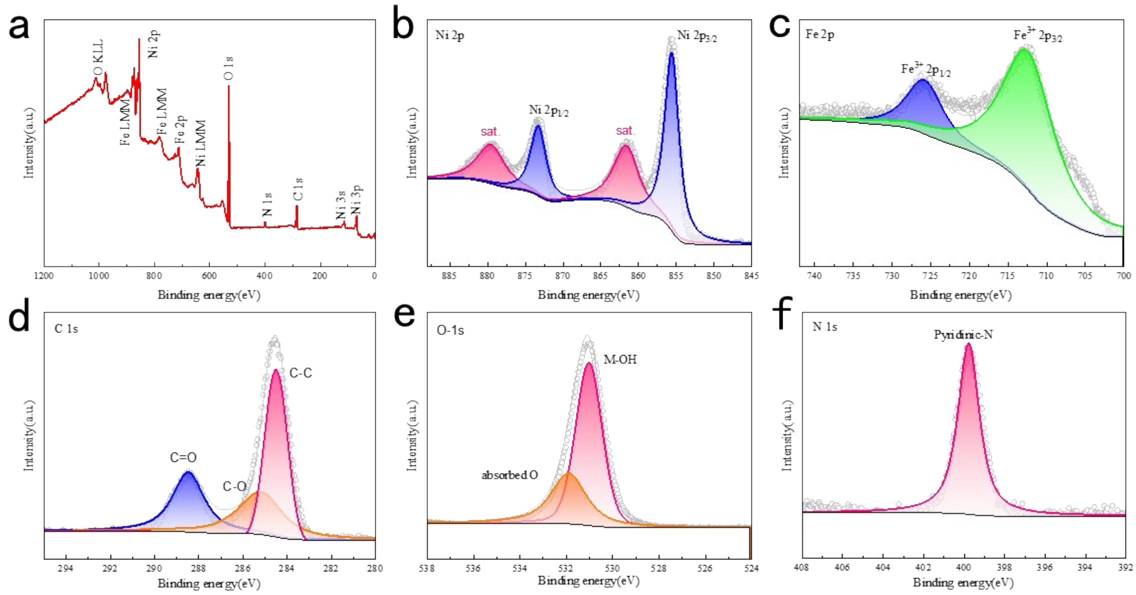


**Fig. S14.** High-resolution XPS spectra of the NiFe LDH@MOF-3 (a) Survey spectrum, (b) Ni 2p, (c) Fe 2p, (d) C 1s, (e) O 1s, (f) N 1s.

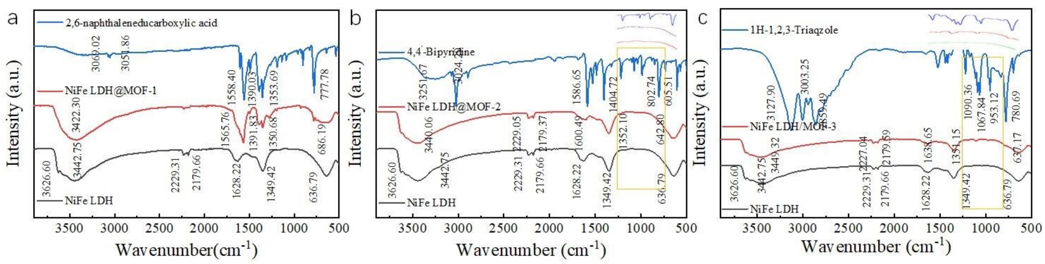


**Fig. S15.** FT-IR spectra of (a) NiFe LDH@MOF-1, (b) NiFe LDH@MOF-2, (c) NiFe LDH@MOF-3.

**Table S1.** Comparison of the OER performance of our NiFe LDH@MOF with other advanced electrocatalysts

| **Catalyst** | **Electrolyte** | **Current density ($j$,mA $cm^{-2}$)** | **Overpotential (mV vs.RHE)** | **References** |
|---|---|---|---|---|
| **NiFe LDH@MOF-1** | 1M KOH | 100 | 266 | this work |
| **NiFe LDH@MOF-2** | 1M KOH | 100 | 252 | this work |
| **NiFe LDH@MOF-3** | 1M KOH | 100 | 242 | this work |
| **5-cycle NiFe LDH** | 1M KOH | 50 | 259 | Electrochim. Acta, 389 (2021) 138523. |
| **S-NiFe LDH exch 0.005M $(NH_4)_2SO_4$** | 1M KOH | 50 | 288 | Chem. Eng. J. 426 (2021) 130873. |

| | | | | |
|---|---|---|---|---|
| **NiFe-LDH@OMC/CC** | 1M KOH | 100 | 296 | Appl. Surf. Sci. 565 (2021) 150533. |
| **NiFe-LDH@NCP+CB(PVP 0.3)** | 1M KOH | 10 | 193 | Int. J. Hydrog. Energy, 47 (2022) 19609–19618. |
| **NiFe-LDH/rGO@NF** | 1M KOH | 50 | 277 | Int. J. Hydrog. Energy, 47 (2022) 8786–8798. |
| **NiFe LDH-PANI** | 1M KOH | 100 | 270 | J. Alloys Compd. 901 (20220 163510. |
| **$Ni_XFe_{1-X}S$** | 1M KOH | 10 | 122 | Appl. Catal. B, 297 (2021) 120453. |
| **Co-CH@NiFe-LDH/NF** | 1M KOH | 20 | 188 | Appl. Catal. B, 304 (2022) 120937. |
| **NiFe LDH/GQDs** | 1M KOH | 10 | 189 | Ultrason Sonochem 76 (2021) 105664. |
| **NiFe LDH/GF** | 1M KOH | 50 | 214 | Chem. Eng. J. 422 (2021) 130123. |
| **NiFe LDH/FeOOH** | 1M KOH+0.5M NaCl | 100 | 286.2 | Nano Energy, 84 (2021) 105932. |
| **NiFe LDH@NiFe** | 1M KOH | 10 | 201 | Inorg. Chem. 60 (2021) 12703–12708. |
| **NiFeOP** | 1M KOH | 10 | 310 | Inorg. Chem. 60 (2021) 17371–17378. |
| **NiFe LDH/NF-36h** | 1M KOH | 20 | 231 | ACS Appl. Mater. Interfaces, 4 (2021) 9022–9031. |
| **V-NiFe LDH** | 1M KOH | 10 | 195 | ACS Sustain. Chem. Eng. 9 (2021) 9436–9443. |
| **Co@NiFe-LDH** | 1M KOH | 10 | 253 | CrystEngComm, 24 (2022) 1573–1581. |
| **CoFe@NiFe-200/NF** | 1M KOH | 10 | 190 | RSC Adv. 11 (2021) 37624–37630. |
| **v-NiFe LDH** | 1M KOH | 50 | 260 | J. Mater. Chem. A 9 (2021) 23697–23702. |

| | | | | |
|---|---|---|---|---|
| **$Ni^{vac}Fe^{vac}$-LDH** | 1M KOH | 100 | 363 | J. Mater. Chem. A 10 (2022) 5244–5254. |
| **NiFe-LDH@Mo-$NiS_2$-NiS/NF** | 1M KOH | 50 | 261 | Appl. Catal. B 253 (2019) 131–139. |
| **NiFe-LDH@Ni-MOF/NF** | 1M KOH | 100 | 248 | Nano Energy 81 (2021) 105606. |
| **FeNi LDH/MOF** | 1M KOH | 100 | 272 | Angewandte Chemie. 133 (2021) 24817–24824. |
| **NiFe LDH@$SnO_2$/NF** | 1M KOH | 10 | 234 | Mater. Today Energy 23 (2022) 100906. |
| **NiMoP@NiFe-LDH** | 1M KOH | 150 | 299 | Mater. Res. Lett. 10 (2022) 88–96. |
| **$Ni_5P_4$/$Ni_2P$/NiFe LDH** | 1M KOH | 100 | 243 | J. Mater. Chem. A 6 (2018) 13619–13623. |
| **10-NiFe LDH/CNTs** | 1M KOH | 10 | 234 | Appl Clay Sci 216 (2022) 106360. |
| **NiFe LDH@ITO** | 1M KOH | 10 | 240 | ACS Sustain. Chem. Eng. 9 (2021) 9436–9443. |
| **$Co_9S_8$@NiFe LDH** | 1M KOH | 10 | 220 | J. Mater. Chem. A 9 (2021) 23697–23702. |

**Electrochemical calculation**

A general mechanism for the OER on oxides in alkaline solution can be summarized as follow[1]：

①$M+OH^- \rightarrow M\text{-}OH_{ads}+e^-$

②$M\text{-}OH_{ads}+OH^- \rightarrow M\text{-}O_{ads}+H_2O+e^-$

③$M\text{-}O_{ads}+M\text{-}O_{ads} \rightarrow 2M+O_2$

④$M\text{-}OH_{ads}+2OH^- \rightarrow M\text{-}OOH_{ads}+H_2O+e^-$

⑤$M\text{-}OOH_{ads}+OH^- \rightarrow M+O_2+H_2O+e^-$

③ has a smaller thermodynamic barrier than the ④⑤ process, so ①②③ is thermodynamically more favorable.

Calculation of the Turnover Frequency[2]：

$$\mathrm{TOF}=\frac{\frac{Number\ of\ total\ oxygen\ turnovers}{cm2}\ of\ genmetric\ area}{\frac{Number\ of\ active\ sites}{cm2}\ of\ geometric\ area}$$

The total number of oxygen turnovers per current density：

$$\mathrm{No.\ of\ O_2}=(per\frac{mA}{cm2})(\frac{1C\bullet s-1}{1000mA})(\frac{1\ mol\ of\ e}{96485.3C})(\frac{1\ mol\ of\ O2}{4\ mol\ of\ e})(\frac{6.022\times 1023\ O2\ molecules}{1mol\ of\ O2})$$

$$=1.56\times 10^{15}\frac{O2\ s-1}{cm2}per\frac{mA}{cm2}$$

Using the assumption that either Ni or Fe acts as active site, the active sites per surface area：

$$\text{Active sites per ECSA}=(\frac{2\ atoms\ unit\ cell-1}{182.94\text{Å}\ unit\ cell-1})^{2/3}$$

$$=4.93\times 10^{14}\ \text{atoms cm}^{-2}{}_{\text{ECSA}}$$

Finally, the plot of current densities is converted into a TOF plot：

$$\mathrm{TOF}=\frac{(1.56\times 1015\frac{O2\ s-1}{cm2}per\frac{mA}{cm2})|j|}{(active\ sites\ per\ surface\ area)\times ECSA}$$

$$=\frac{(1.56\times 1015\frac{O2\ s-1}{cm2}per\frac{mA}{cm2})|j|}{(4.93\times 1014\ atoms\ per\ ECSA)\times ECSA}$$

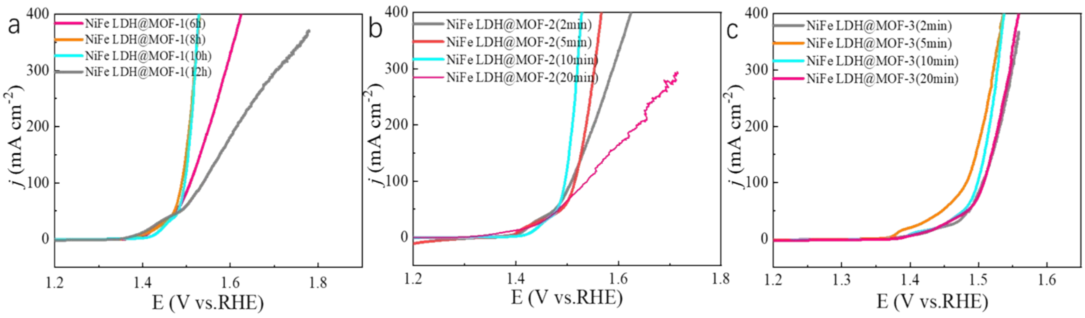


**Fig. S16.** LSV curves of NiFe LDH@MOF-1, NiFe LDH@MOF-2 and NiFe LDH@MOF-3 at different reaction period.

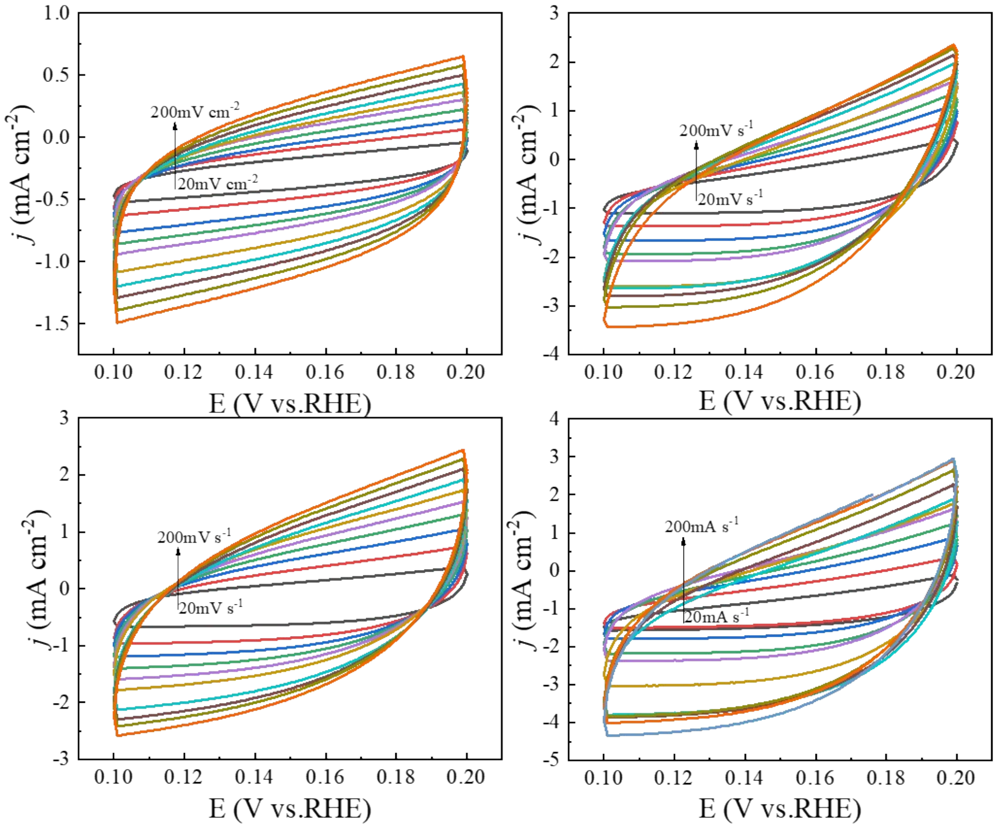


**Fig. S17.** Cyclic voltammetry at potential range without faradaic ion adsorption and desorption process for (a) NiFe LDH, (b) NiFe LDH@MOF-1, (c) NiFe LDH@MOF-2 and (d) NiFe LDH@MOF-3.

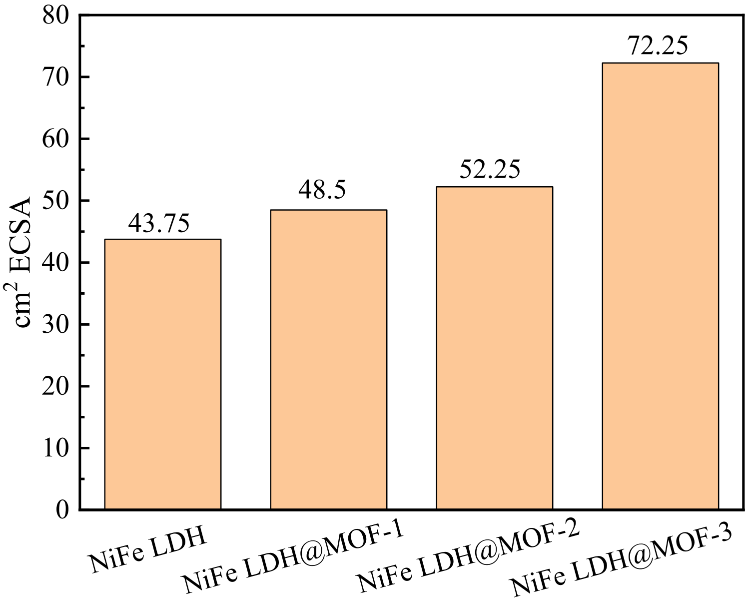


**Fig. S18.** Comparison of the electrochemical active surface area (ECSA) of NiFe LDH and NiFe LDH@MOFs.

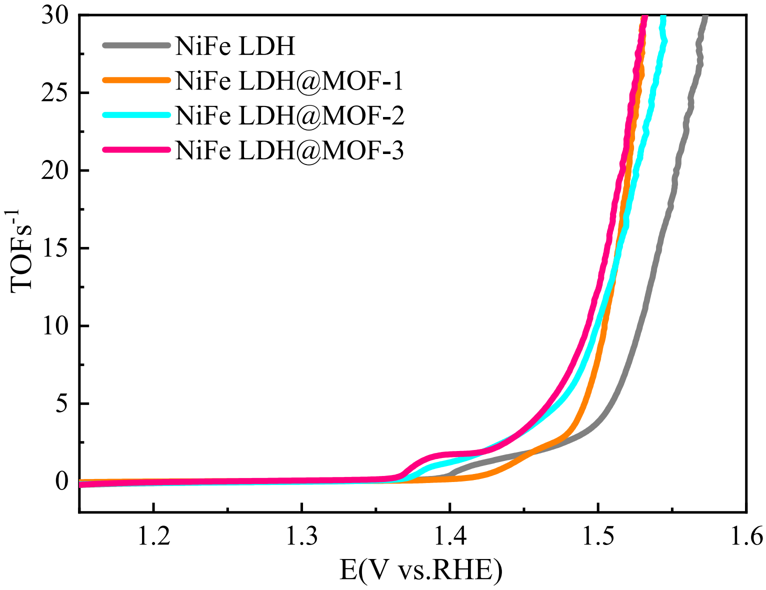


**Fig. S19.** TOF as a function the overpotential for NiFe LDH, NiFe LDH@MOF-1, NiFe LDH@MOF-2 and NiFe LDH@MOF-3.

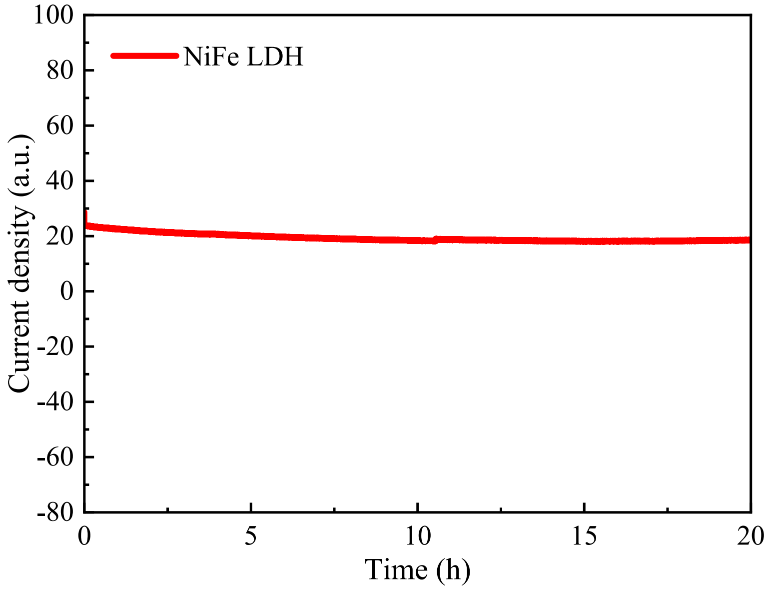


**Fig. S20.** The long-term stability of NiFe LDH.

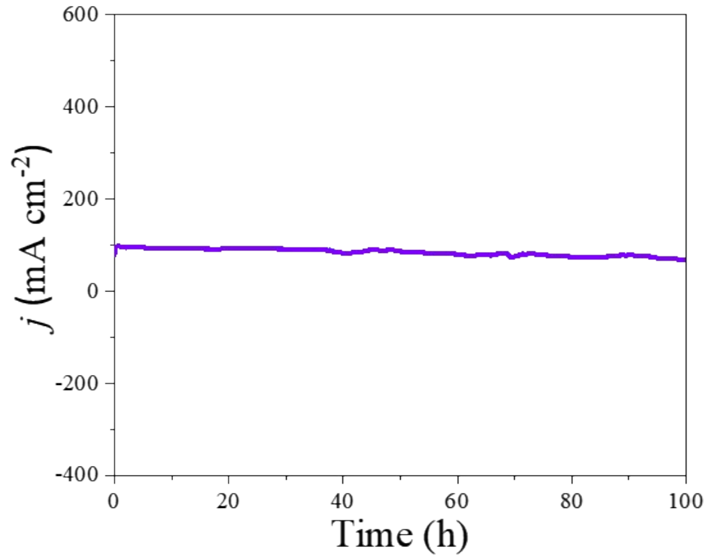


**Fig. S21.** Stability test for NiFe LDH@MOF-3 electrode at constant current density of 100 mA $cm^{-2}$ in 1M KOH at 25 °C.

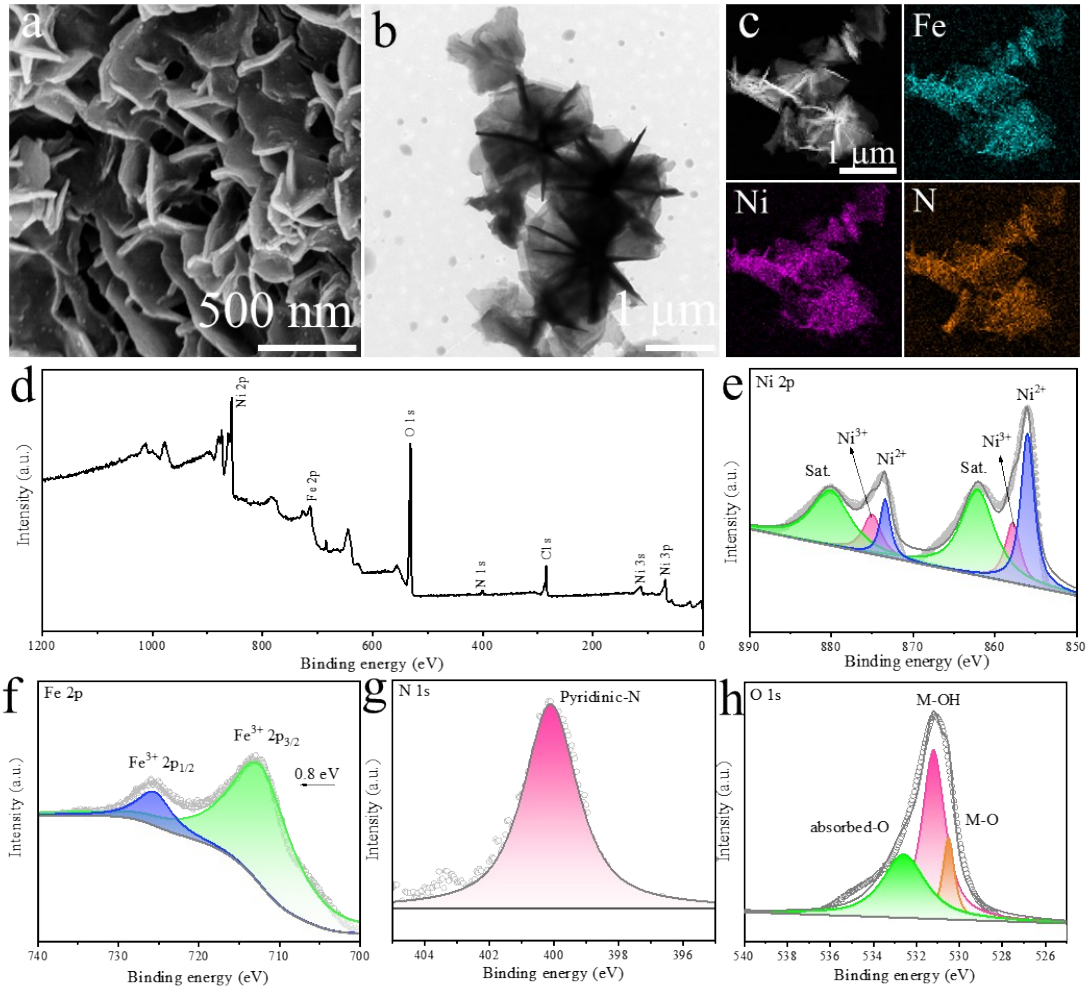


**Fig. S22** (a) SEM image, (b) TEM image, (c) STEM image and elemental mappings, (d) Survey spectrum, (e) Ni 2p, (f) Fe 2p, (g) N 1s, (h) O 1s spectra of NiFe LDH@MOF-3 after OER test.

[Quantitative Result] NiFe LDH

| Analyte | Result | Proc-Calc | Line | Net Int. | BG Int. |
|---|---|---|---|---|---|
| NiO | 81.9059 % | Quant.-FP | NiKa | 615.237 | 2.711 |
| Fe2O3 | 18.0941 % | Quant.-FP | FeKa | 205.771 | 1.651 |

NiFe LDH@MOF-1

| Compound | m/m% | StdErr | El | m/m% | StdErr |
|---|---|---|---|---|---|
| NiO | 63.12 | 0.24 | Ni | 49.60 | 0.19 |
| Fe2O3 | 35.74 | 0.35 | Fe | 24.99 | 0.25 |

NiFe LDH@MOF-2

| Compound | m/m% | StdErr | El | m/m% | StdErr |
|---|---|---|---|---|---|
| NiO | 61.59 | 0.24 | Ni | 48.40 | 0.19 |
| Fe2O3 | 38.37 | 0.24 | Fe | 26.83 | 0.17 |

NiFe LDH@MOF-3

| Compound | m/m% | StdErr | El | m/m% | StdErr |
|---|---|---|---|---|---|
| NiO | 63.08 | 0.24 | Ni | 49.57 | 0.19 |
| Fe2O3 | 36.78 | 0.28 | Fe | 25.73 | 0.20 |

**Fig. S23.** WDXRF data of NiFe LDH, EDXRF data of NiFe LDH@MOF-1, NiFe LDH@MOF-2 and NiFe LDH@MOF-3.

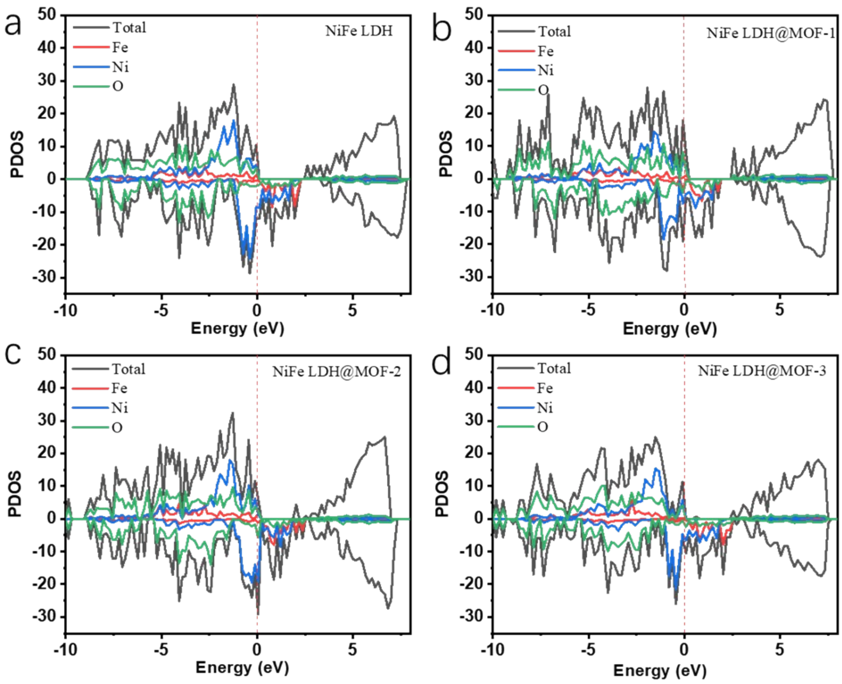


**Fig. S24.** The PDOS of (a) NiFe LDH, (b) NiFe LDH@MOF-1, (c) NiFe LDH@MOF-2, and (d) NiFe LDH@MOF-3.

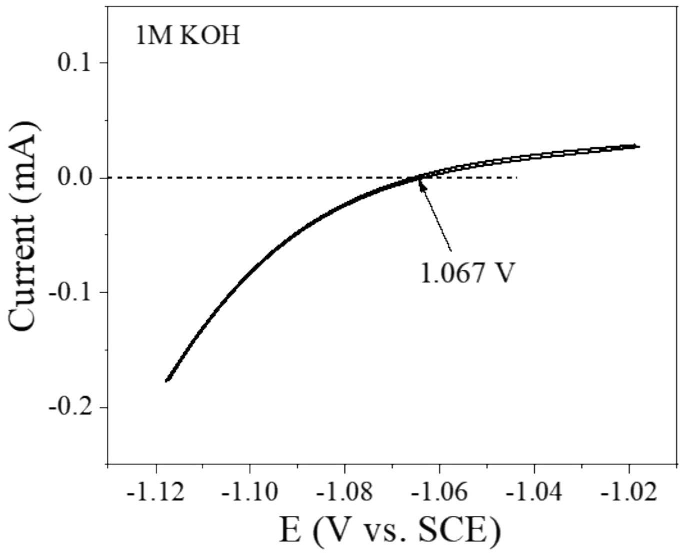


**Fig. S25.** Calibration of SCE reference electrode to RHE (1.0 M KOH).

Calibration of SCE reference electrode with respect to reversible hydrogen electrode (RHE) with a scan rate of 1 mV/s in $H_2$ saturated 1.0 M KOH electrolyte. The measured value of 1.067 V is closed to the calculated value of 1.068 V.

**References:**

[1] F. Song, M. M. Busch, B. Lassalle-Kaiser, C. S. Hsu, E. Petkucheva, M. Bensimon, H. Chen, C. Corminboeuf, and X. Hu, *ACS Cent. Sci.,* 2019, **5**, 558–568.

[2] Y. Luo, Y. Wu, D. Wu, C. Huang, D. Xiao, H. Chen, S. Zheng, P. Chu, *ACS Appl. Mater. Interfaces,* 2020, **12**, 42850–42858.